

# **Dosimetric impact of intrafraction rotations in stereotactic prostate radiotherapy: A subset analysis of the TROG 15.01 SPARK trial**

Joshua Wolf<sup>1</sup> MSc, Joshua Nicholls<sup>1</sup> BMRS, Perry Hunter<sup>1</sup> BMRS, Doan Trang Nguyen<sup>2</sup> PhD, Paul Keall<sup>2</sup> PhD, Jarad Martin<sup>1</sup> PhD

<sup>1</sup>Calvary Mater Newcastle, New South Wales, Australia

<sup>2</sup>ACRF Image -X Institute, University of Sydney, New South Wales, Australia

## **Corresponding Author/Statistical Analyst Contact Details:**

Joshua Wolf

Radiation Oncology Department

Calvary Mater Newcastle

Waratah, NSW, Australia, 2298

[Joshua.Wolf@calvarymater.org.au](mailto:Joshua.Wolf@calvarymater.org.au)

Phone: +61423316854

## **Source of Financial Support:**

SPARK is funded by both Cancer Australia and the Prostate Cancer Foundation of Australia

**Conflicts of Interest:** None

# Abstract

## Background & Purpose

Accurate delivery of radiotherapy is critical to achieve optimal treatment outcomes. Interfraction translational IGRT is now standard, and intrafraction motion management is becoming accessible. Some platforms can report both translational and rotational movements in real time. This study aims to quantify the dosimetric impact of observed intrafraction rotation of the prostate measured using monitoring software.

## Materials & Methods

A dose grid resampling algorithm was used to model the dosimetric impact of prostate rotations for 20 patients on a SBRT prostate clinical trial. Translations were corrected before and during treatment, but rotations were not. Real time rotation data was acquired using KIM and a cumulative histogram analysis performed. Prostate volumes were rotated by the range of observed angles and used to calculate DVH data.

## Results

The pitch axis had a higher range of observed rotations resulting in only 7 patients spending at least 90% of the beam on time across all fractions within rotation angles resulting in PTV D95% $\geq$ 36Gy in this axis. The yaw and roll axes saw 17 and 15 patients respectively achieving this criterion. All but one of 20 patients exceeded CTV D98% $\geq$ 36Gy for all observed rotation angles.

## Conclusions

Current CTV-PTV margins do not result in compromised CTV dose coverage due to inter and intrafraction prostate rotations in the absence of other uncertainties. Reduced PTV dosing is due to the extremely conformal treatment delivery but is unlikely to be clinically deleterious. Prostate standard IGRT should continue to focus on correcting any observed translational movements. Margin reduction could be explored in conjunction with other uncertainties.

## Highlights

- Prostate intrafraction rotations are typically non-symmetrical about the pitch axis
- Observed rotations resulted in reduced PTV dose coverage for many patients
- CTV coverage was maintained for virtually all observed rotations
- Existing SBRT CTV-PTV margins sufficient to account for intrafraction rotations

## Keywords

Intrafraction rotations, SBRT, prostate, dosimetry

# Introduction

The use of ultra-hypofractionated, or SBRT, treatments of the prostate has gained in popularity in recent years.<sup>1-3</sup> Due to the inherent dose per fraction escalation of these approaches, there is a need for high dose gradients to be employed with tighter than conventional margins. Along with the low number of fractions being used, this results in an increased need for high quality image guidance to be employed to ensure accurate treatment delivery. While commonly used systems such as Cone Beam CT (CBCT) give reasonable image quality and a high level of positioning accuracy when used with implanted fiducial markers, they only provide a snapshot of the position of the prostate. Studies have shown that the prostate can undergo both translational and rotational movements over the timespan of a single fraction delivery.<sup>4-6</sup> Where decreased CTV-PTV margins are employed there is an increased risk that geometric misses will occur due to these movements.<sup>7</sup> As such it has been identified that it would be ideal to be able to monitor the relative orientation and location of the prostate in real time during the treatment. This information might be used for example to gate the beam or to adapt the treatment delivery in real time in the case of tumor tracking.<sup>8,9</sup>

To address this need, several platforms have been developed to enable real time tumor position monitoring. Some of the earliest approaches to this were to utilize the MV imaging systems typically integrated on modern linacs to monitor the location of implanted fiducials within the beam portal throughout the treatment delivery.<sup>10,11</sup> One significant limitation to this approach however has come with the widespread adoption of IMRT and VMAT delivery techniques which can obscure some, or all, of the nominal beam portal throughout the delivery. More recently 3D systems independent of the treatment unit such as the Calypso system (Varian Medical Systems, Palo Alto, USA) have been developed.<sup>12</sup> Calypso utilizes implanted radiofrequency transponders which are excited and in turn detected using a large electromagnetic array panel. While Calypso achieves good positional accuracy and precision, it does require the use of extra external equipment in addition to the transponders.<sup>13</sup> To address this limitation it would be ideal to utilize a tumor monitoring platform which only utilizes the existing widely available on-board imaging options.

Kilovoltage Intrafraction Motion (KIM) collects kV data in real time, segments prostatic fiducial positioning, and provides a real-time output of the translational and rotational prostate positions to the Linac treatment console.<sup>14</sup> The TROG 15.01 SPARK clinical trial sought to verify the translational dosimetric accuracy of KIM for the delivery of 36.25Gy in five fractions of SBRT for men with low-intermediate risk disease.<sup>15</sup> The current study aims to describe the dosimetric impact of rotational intrafraction motion on both the CTV and PTV in SBRT treatments of the prostate.

## Methods and Materials

### Planning & Treatment

A total of 20 patient treatments were investigated which consisted of 100 fractions treated on the TROG 15.01 SPARK trial at a single center.<sup>15</sup> In brief summary, the CTV was the prostate, and a 5mm CTV to PTV expansion in all directions except posterior where 3 mm was used. These patients were planned to receive 36.25 Gy in 5 fractions to the PTV using two near complete VMAT arcs with treatment delivered on a Varian TrueBeam with a 10 MV Flattening Filter Free (FFF) 2400MU/minute

beam. All translational motions were corrected prior to treatment, and any movement of >2mm sustained for >5s in any axis led to a gating event.

### **KIM Data**

During treatment delivery, the translational and rotational deviations from the reference position of three implanted markers were tracked using KIM.<sup>16</sup> This KIM rotation data represents the angle by which the 3D reference positions of the three implanted fiducial markers need to be rotated by in order to reach the measured fiducial position as described by Tehrani *et al.*<sup>17</sup> While the data generated by the KIM software represents a series of chained extrinsic rotations (pitch, roll and yaw), for this analysis each axis was independently analyzed as a first order effect investigation of the dosimetric impact of rotations on the prostate. A cumulative histogram analysis was performed to assess the proportion of time each patient's prostate was rotated by less than a given angle using all the rotation data points measured during beam-on throughout their treatments.

### **Rotation Modelling**

Because patients are initially set up using IGRT utilizing translational shifts alone, leaving any measured rotations unchanged, it is postulated that the 3D dose distribution around the isocenter should remain relatively consistent regardless of prostate rotation due to the relatively uniform tissue composition in this region for the prostate. As such, the dose received by a rotated prostate within this aligned outer body volume should be able to be estimated by virtually rotating the CTV and PTV structures about the fiducial centroid and sampling the planned 3D dose grid. This sampled dose data can be then used to create a DVH curve. Consequently, both CTV D98% and PTV D95% were determined from the reconstructed DVH. If this analysis is done for a range of angles in each axis it is possible to identify edge cases at which rotations result in sub-optimal dose distributions. This process is summarized in Figure 1 with an example of how a result is calculated.

### **MATLAB Scripting**

A custom MATLAB (The MathWorks Inc., Natick, USA) script was formulated to perform both of the above analyses (rotation data cumulative histogram and DVH parameters with rotation angle). The proportion of time each patient's prostate was within a rotation angle in each axis, which results in CTV D98% $\geq$ 36 Gy and PTV D95% $\geq$ 36Gy, was calculated.

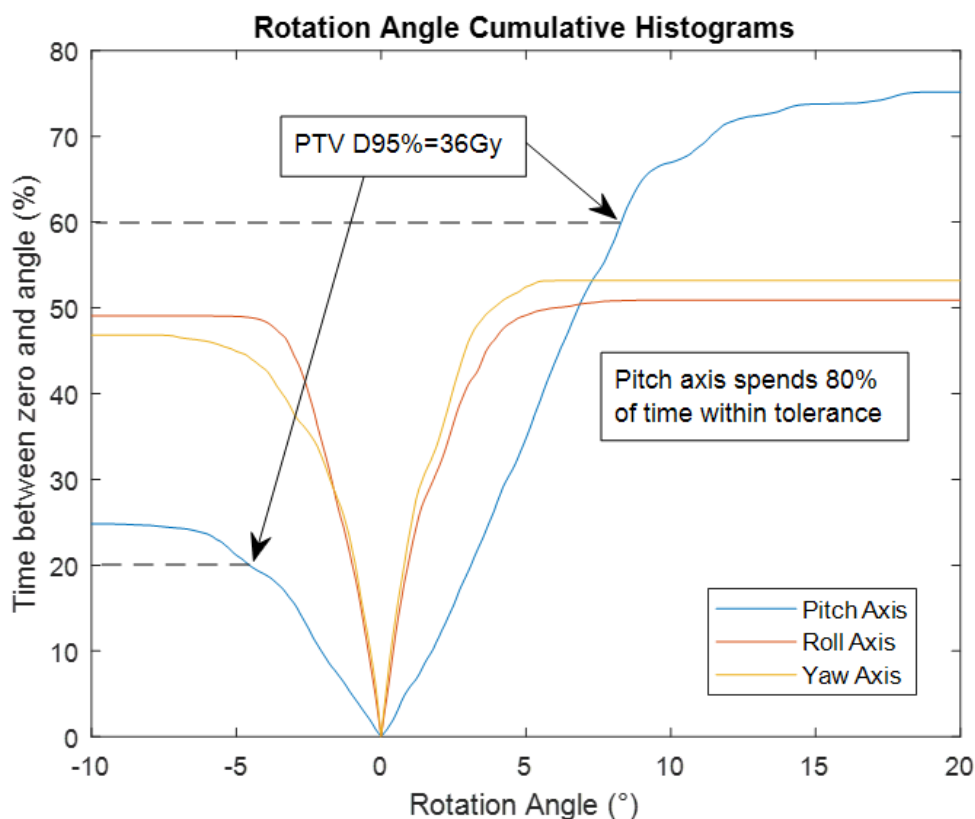
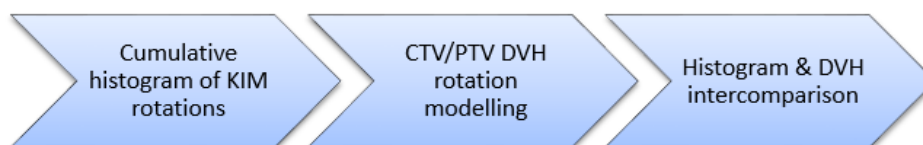


Figure 1. Workflow process of this study along with worked example. Rotation data from KIM is first analyzed to generate a cumulative angle distribution about zero degrees. Next the PTV and CTV are rotated through these angles to calculate the delivered DVH throughout the treatment. Finally these two data sets are compared to find the proportion of time the patient spends within rotation angles resulting in acceptable DVH results and compared to the 90% tolerance.

This script also analyzed the CTV and PTV volumes themselves as well as the 3D dose distribution in order to assess the sphericity and conformity index for each structure. The sphericity was defined as by Waddel as the ratio of the surface area of a sphere (with the same volume as the structure) to the surface area of the structure in question.<sup>18</sup> The sphericity of a sphere is 1 by definition and is less than 1 for all other shapes. The conformity index, or CI, is defined as the ratio of the volume of the 95% isodose line to the volume of the structure and is a measure of how over-covered the structure is by the prescription dose. Combined, it is expected that these metrics will have some predictive value of the dosimetric sensitivity of a given patient's plan to rotations in each axis.

## Results

### Observed Rotations

The minimum, maximum, mean and standard deviation of the rotation angles was calculated using all the KIM data for all patients, these are presented in Table 1. In the pitch axis there is a systematic rotation noted which is absent in the roll and yaw axes. Concurrently, the range and standard deviation of rotational angles is larger in the pitch axis. This data is graphically represented in Figure 2, showing the distribution of prostate rotation angles in each of the three axes, which demonstrates an asymmetric distribution and extreme rotation beyond 15 degrees in some instances.

Table 1. Mean, standard deviation and range of all KIM measured data for each rotation axis.

Axis	Mean Angle	St Dev	Min Angle	Max Angle
Pitch	3.6 °	4.9 °	-9.6 °	19.1 °
Roll	0.2 °	2.1 °	-7.7 °	9.4 °
Yaw	0.1 °	2.1 °	-8.7 °	5.9 °

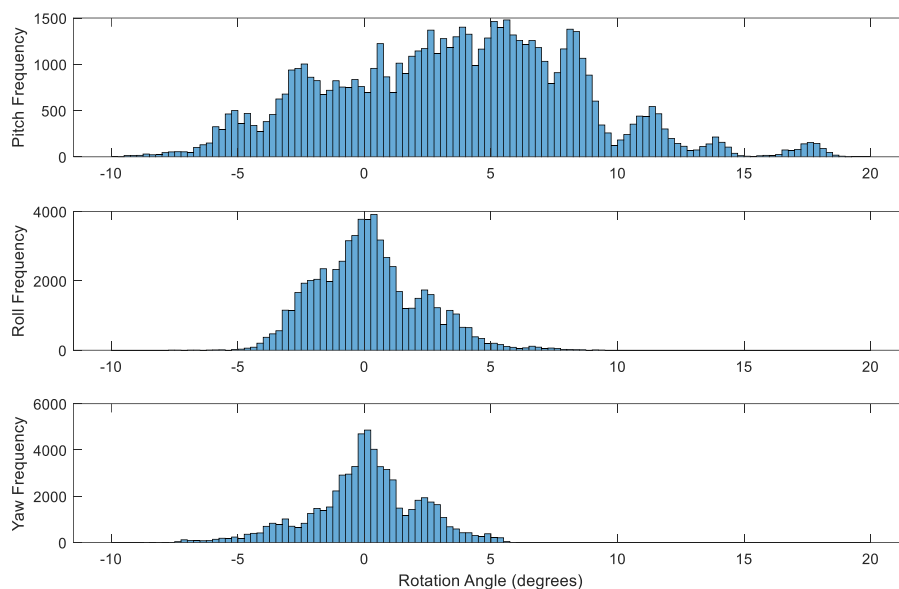


Figure 2. Distributions of all measured rotations for all patients in study for each axis.

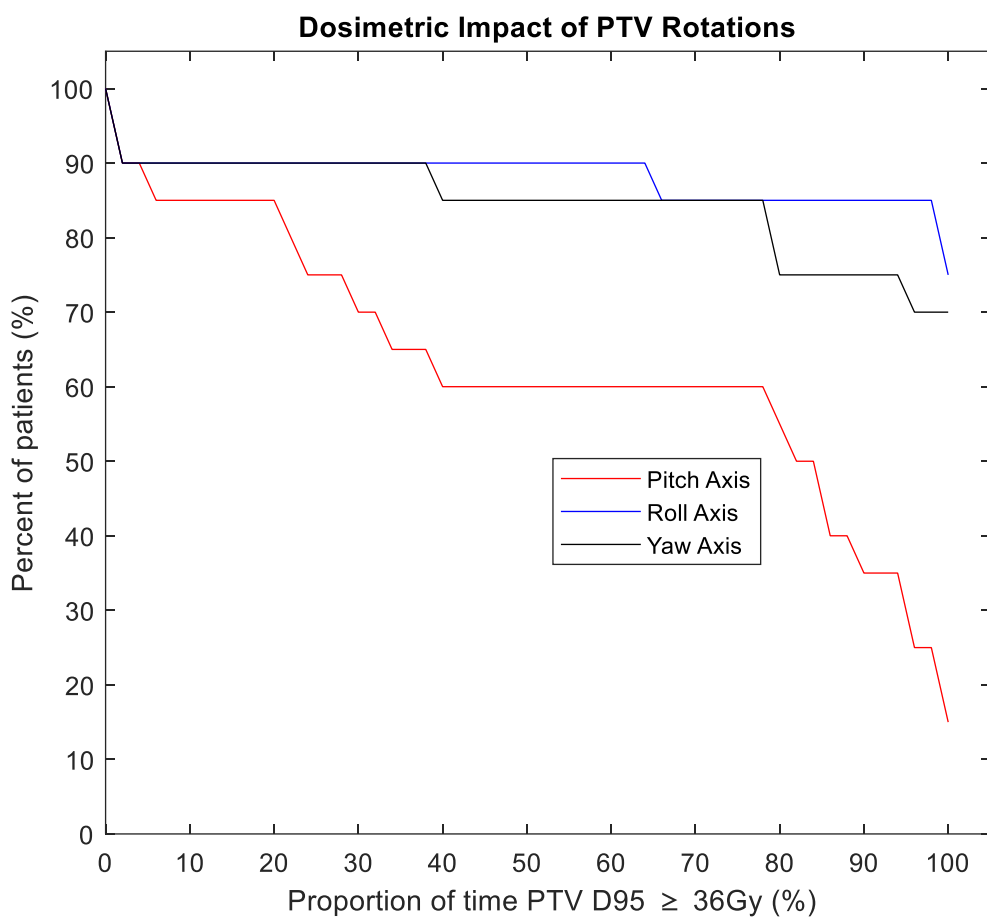
### Modelled Dose Coverage

For the entire cohort of 20 patients the mean sphericity and CI was calculated along with the number of patients who spent at least 90% of beam on time within rotations resulting in an acceptable DVH result. This was defined as PTV D95%  $\geq$  36 Gy and CTV D98%  $\geq$  36 Gy as these were the major variation tolerances in the SPARK trial. These results can be seen in Table 2. It should be noted that two patients in the cohort had such conformal doses that any rotation of the prostate would result in a sub-standard PTV DVH result, however even for these patients the CTV was within acceptable rotations 100% of the time with the exception of a single patient in the pitch axis.

Table 2. Mean and standard deviation of sphericity and conformity index across all patient for CTV and PTV along with number of patients spending at least 90% of their treatment within rotation angles resulting in acceptable DVH results.

Structure	Sphericity		Conformity Index		Number of patients within 90% (out of 20)		
	Mean	StDev	Mean	StDev	Pitch	Roll	Yaw
CTV	0.79	0.03	2.32	0.22	19	20	20
PTV	0.83	0.02	1.19	0.05	7	17	15

The proportion of patients spending at least a given proportion of time above protocol compliant PTV and CTV dose coverage is shown in Figure 3a and Figure 3b respectively. The pitch axis had the largest dosimetric impact of all three axes with most patients spending a high proportion of time at rotation angles large enough to compromise the coverage of the PTV with 95% of the prescription dose.



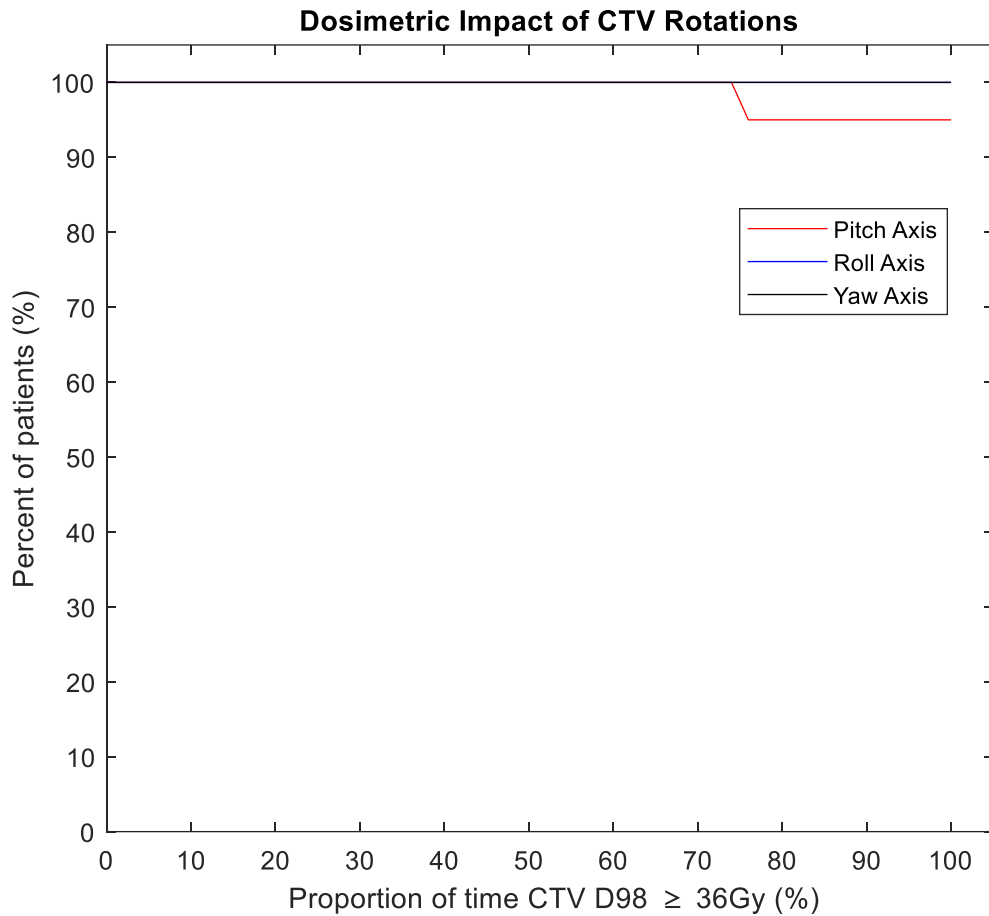


Figure 3a & 3b. Proportion of patients spending at least a given proportion of time within rotations resulting in acceptable PTV and CTV DVH results respectively for each axis of rotation.

## Discussion

Our data suggests that the dosimetric impact of intrafractional rotation is minimal to the prostate in the context of the 3-5 mm CTV-PTV margins used on this trial. It should be noted that as a first order approximation, this analysis has not accounted for the full influence of other uncertainties accounted for in the CTV-PTV margin such as delineation and seed localization errors. This has implications for future IGRT strategies as well as margin generation.

It is remarkable to reflect on the rapid progressions in research and technology in prostate radiotherapy, with the latter sometimes reaching implementation prior to rigorous assessment. The adoption of conventional dose escalation prior to moderately hypofractionated radiotherapy as a transition towards SBRT is on the background of large, randomized controlled trials.<sup>19-21</sup> Conversely, technical innovations such as integration of IMRT, IGRT and MRI have been widely adopted, but more based on surrogate endpoints such as dosimetry and accuracy.<sup>22-24</sup> The clinical release of innovations such as real time rotation and MRI Linacs threaten to outstrip through assessment on how to optimally integrate them.<sup>25</sup> This will remain an ongoing challenge for our specialty.



We observed an asymmetric distribution of prostate rotations in this patient cohort, primarily in the pitch axis. This leads to much poorer dosimetric results in the PTV for this axis. Pitch can be thought of as a tilt in the longitudinal plane. As such, any alterations in rectal volume would be expressed by changes in the pitch axis. In particular, given the delay between initial patient positioning and treatment commencement, rectal filling from the proximal direction may be the cause of the systemic positive shift noted in this axis. This systematic difference between planning and treatment may have been affected by progressively greater adherence to the bowel preparation as the patient progressed through the treatment journey. To minimize this, we recommend close attention to an empty bowel protocol prior to both planning and treatment, and reducing the time from initial set-up to commencement of treatment. Similarly with the increasing inclusion of the seminal vesicles in the target volume in recent trials will also further increase the dosimetric impact of these prostate tilts due to the elongation of the volume in the superior-inferior direction.<sup>26</sup>

It can be seen that for both CTV and PTV the sphericity and CI are highly regular with very low variability. This would indicate that the patient population have very similar shaped prostates and that consistent planning outcomes are being achieved respectively. In particular, a near spherical prostate would be relatively insensitive to any rotations given the symmetry of such a volume. There is no clear correlation between the sphericity or CI of patients who scored poorly and the proportion of time spent within acceptable rotation bounds. Given our patients had low to intermediate risk disease; seminal vesicles were not systematically treated. If this were the case, the sphericity would be less for such cases, and rotational motions may have a greater dosimetric impact.

Other studies investigating the impact of prostate rotations have tended to focus on the dosimetric changes to the PTV and when we look at this data it does appear that these rotations have an effect on the dose coverage of the prostate<sup>27-29</sup>, with rotations in the pitch axis generally being the primary component.<sup>30</sup> However, the CTV-PTV margin is meant to take motions such as these, as well as other factors including delineation error, into account in order to ensure adequate coverage of the CTV. For delineation, the use of a single observer for all contouring with a known variation of approximately 1-2mm on MRI will reduce the impact of this error, and the control for real time translational error should also reduce uncertainty.<sup>22,31</sup> Residual errors relating to factors such as seed positioning and hardware performance are likely to be small, but this analysis was not designed to fully investigate these. The uniformly good CTV results found in this study indicate that the margins currently applied in these patients are likely to be adequate. Interestingly, these margins were even able to compensate for the observed systematic shift in the pitch axis observed in the patient cohort between the planning imaging appointment and the treatment fractions. As such it is likely to be inappropriate to only look at PTV dose coverage when accounting for the impact of observed prostate rotations.

While 6 degrees of freedom (DoF) couches which allow online correction of tumor rotations are becoming more common on new linacs there are still many centers around the world which have only translational shifting capabilities. Even where these 6 DoF couches are available it is rare to have any sort of real time tumor rotation measurement capability such as that afforded by the KIM software.<sup>14</sup> This work helps to illustrate that the realistic ranges of prostate rotations encountered in the clinic are unlikely to cause sub-par dosimetric outcomes where only the translational shifts have been applied as in traditional IGRT. As such, our findings will be reassuring to centers as real

time rotational data as well as methods to respond to it become more widely implemented, that translational IGRT is likely to remain the standard of care.

While this work has focused on SBRT prostate treatments, this approach may be equally applicable to other sites with relatively spherical tumors which might suffer from tumor rotation and deformation throughout the treatment which could traditionally be accounted for with a margin. Examples include lung or liver tumors.

The methodology utilized here has three key assumptions which have been made to simplify the modelling process. The first of these is the use of the reported rotation around each axis independent of the other axes. Due to the complex interplay encountered when combining rotations around different axes this approach was taken to enable the methodology used here. Translational shifts were corrected prior to treatment delivery in the SPARK trial with only the rotations remaining uncorrected and as such the external contour of the patient is likely to be very similar to that planned. Thus the assumption has been made that the gross 3D dose distribution across the entire pelvis remains the same regardless of the prostate rotation. Finally it has been assumed that the PTV, and thus the CTV contained within it, rotates rigidly about the measured rotation centroid. Due to the relatively uniform nature of the prostate region and low rotation angles measured it was felt that this was a good first order approximation for these last two assumptions.

Future work in this area should focus on investigating the interplay of the various rotation axes with each other and ideally utilize prostate deformation models instead of rigid rotations to more accurately model the actual patient situation. In addition the dosimetric impact of reducing the CTV-PTV margin should be prospectively performed to find the optimal margin required to account for the prostate rotations observed in the patient population.<sup>32</sup> Given that the posterior prostate margin is most likely to be compromised by pitch, and yet at only 3mm it was adequate in our study for CTV dosimetric coverage, our successor prostate SBRT trial will adopt uniform 3mm CTV-PTV margins.

## Conclusions

The 3mm-5mm CTV-PTV expansion margins applied for SBRT prostate patients on the SPARK clinical trial are adequate to account for the observed intrafraction rotations of the prostate with minimal impact on modelled CTV dosimetry where other uncertainties such as hardware performance are ignored. It may be appropriate to reduce these margins given the current IGRT technology available and rotation angles observed in these patients. Adjustments for prostate rotations do not appear to be of dosimetric benefit.

## References

1. King CR, Freeman D, Kaplan I, et al. Stereotactic body radiotherapy for localized prostate cancer: pooled analysis from a multi-institutional consortium of prospective phase II trials. *Radiotherapy and oncology : journal of the European Society for Therapeutic Radiology and Oncology* 2013;109:217-21.
2. Katz AJ, Kang J. Stereotactic body radiotherapy as treatment for organ confined low- and intermediate-risk prostate carcinoma, a 7-year study. *Frontiers in oncology* 2014;4:240.

3. Alayed Y, Cheung P, Pang G, et al. Dose escalation for prostate stereotactic ablative radiotherapy (SABR): Late outcomes from two prospective clinical trials. *Radiotherapy and oncology : journal of the European Society for Therapeutic Radiology and Oncology* 2018;127:213-8.
4. Bertholet J, Worm ES, Fledelius W, Hoyer M, Poulsen PR. Time-Resolved Intrafraction Target Translations and Rotations During Stereotactic Liver Radiation Therapy: Implications for Marker-based Localization Accuracy. *International journal of radiation oncology, biology, physics* 2016;95:802-9.
5. Thomas SJ, Ashburner M, Tudor GS, et al. Intra-fraction motion of the prostate during treatment with helical tomotherapy. *Radiotherapy and oncology : journal of the European Society for Therapeutic Radiology and Oncology* 2013;109:482-6.
6. Xie Y, Djajaputra D, King CR, Hossain S, Ma L, Xing L. Intrafractional motion of the prostate during hypofractionated radiotherapy. *International journal of radiation oncology, biology, physics* 2008;72:236-46.
7. Litzenberg DW, Balter JM, Hadley SW, et al. Influence of intrafraction motion on margins for prostate radiotherapy. *International journal of radiation oncology, biology, physics* 2006;65:548-53.
8. Keall PJ, Nguyen DT, O'Brien R, et al. The first clinical implementation of real-time image-guided adaptive radiotherapy using a standard linear accelerator. *Radiotherapy and Oncology* 2018.
9. Moorrees J, Bezak E. Four dimensional radiotherapy: a review of current technologies and modalities. *Australas Phys Eng Sci Med* 2012;35:399-406.
10. Keall PJ, Todor AD, Vedam SS, et al. On the use of EPID-based implanted marker tracking for 4D radiotherapy. *Med Phys* 2004;31:3492-9.
11. Mao W, Riaz N, Lee L, Wiersma R, Xing L. A fiducial detection algorithm for real-time image guided IMRT based on simultaneous MV and kV imaging. *Med Phys* 2008;35:3554-64.
12. Nguyen T, Hsu W, Lim M, Naff N. Delivery of stereotactic radiosurgery: a cross-platform comparison. *Neurological research* 2011;33:787-91.
13. Krauss A, Nill S, Tacke M, Oelfke U. Electromagnetic real-time tumor position monitoring and dynamic multileaf collimator tracking using a Siemens 160 MLC: geometric and dosimetric accuracy of an integrated system. *International journal of radiation oncology, biology, physics* 2011;79:579-87.
14. Nguyen DT, O'Brien R, Kim JH, et al. The first clinical implementation of a real-time six degree of freedom target tracking system during radiation therapy based on Kilovoltage Intrafraction Monitoring (KIM). *Radiotherapy and oncology : journal of the European Society for Therapeutic Radiology and Oncology* 2017;123:37-42.
15. Keall P, Nguyen DT, O'Brien R, et al. Stereotactic prostate adaptive radiotherapy utilising kilovoltage intrafraction monitoring: the TROG 15.01 SPARK trial. *BMC cancer* 2017;17:180.
16. Ng JA, Booth JT, O'Brien RT, et al. Quality assurance for the clinical implementation of kilovoltage intrafraction monitoring for prostate cancer VMAT. *Medical physics* 2014;41:111712.
17. Tehrani JN, O'Brien RT, Poulsen PR, Keall P. Real-time estimation of prostate tumor rotation and translation with a kV imaging system based on an iterative closest point algorithm. *Physics in medicine and biology* 2013;58:8517-33.
18. Waddel H. Volume, Shape and Roundness of Quartz Particles. *The Journal of Geology* 1935;43:250-80.
19. Trada Y, Plank A, Martin J. Defining a dose–response relationship for prostate external beam radiotherapy. *Journal of medical imaging and radiation oncology* 2013;57:237-46.
20. Martin JM, Supiot S, Keall PJ, Catton CN. Moderately hypofractionated prostate external beam radiotherapy: an emerging standard. *The British journal of radiology* 2018:20170807.
21. Catton CN, Lukka H, Gu C-S, et al. Randomized trial of a hypofractionated radiation regimen for the treatment of localized prostate cancer. *Journal of Clinical Oncology* 2017;35:1884-90.
22. Khoo EL, Schick K, Plank AW, et al. Prostate contouring variation: can it be fixed? *International Journal of Radiation Oncology• Biology• Physics* 2012;82:1923-9.

23. Ratnayake G, Martin J, Plank A, Wong W. Incremental changes versus a technological quantum leap: The additional value of intensity-modulated radiotherapy beyond image-guided radiotherapy for prostate irradiation. *Journal of medical imaging and radiation oncology* 2014;58:503-10.
24. Ost P, Speleers B, De Meerleer G, et al. Volumetric arc therapy and intensity-modulated radiotherapy for primary prostate radiotherapy with simultaneous integrated boost to intraprostatic lesion with 6 and 18 MV: a planning comparison study. *International journal of radiation oncology, biology, physics* 2011;79:920-6.
25. Bjerre T, Crijns S, af Rosenschold PM, et al. Three-dimensional MRI-linac intra-fraction guidance using multiple orthogonal cine-MRI planes. *Physics in medicine and biology* 2013;58:4943-50.
26. Richardson M, Sidhom M, Gallagher S, et al. PROstate Multicentre External beam radioTHERapy Using a Stereotactic boost: the PROMETHEUS study protocol. *BMC cancer* 2018;18:588.
27. Amro H, Hamstra DA, McShan DL, et al. The dosimetric impact of prostate rotations during electromagnetically guided external-beam radiation therapy. *International journal of radiation oncology, biology, physics* 2013;85:230-6.
28. Deutschmann H, Kametriser G, Steininger P, et al. First clinical release of an online, adaptive, aperture-based image-guided radiotherapy strategy in intensity-modulated radiotherapy to correct for inter- and intrafractional rotations of the prostate. *International journal of radiation oncology, biology, physics* 2012;83:1624-32.
29. Olsen JR, Noel CE, Baker K, Santanam L, Michalski JM, Parikh PJ. Practical method of adaptive radiotherapy for prostate cancer using real-time electromagnetic tracking. *International journal of radiation oncology, biology, physics* 2012;82:1903-11.
30. Litzenberg DW, Muenz DG, Archer PG, et al. Changes in prostate orientation due to removal of a Foley catheter. *Medical Physics* 2018;45:1369-78.
31. Dowling JA, Sun J, Pichler P, et al. Automatic substitute computed tomography generation and contouring for magnetic resonance imaging (MRI)-alone external beam radiation therapy from standard MRI sequences. *International Journal of Radiation Oncology • Biology • Physics* 2015;93:1144-53.
32. Li HS, Chetty IJ, Enke CA, et al. Dosimetric consequences of intrafraction prostate motion. *International journal of radiation oncology, biology, physics* 2008;71:801-12.

## Figure Captions

Figure 1: Workflow process of this study along with worked example. Rotation data from KIM is first analyzed to generate a cumulative angle distribution about zero degrees. Next the PTV and CTV are rotated through these angles to calculate the delivered DVH throughout the treatment. Finally these two data sets are compared to find the proportion of time the patient spends within rotation angles resulting in acceptable DVH results and compared to the 90% tolerance.

Figure 2: Distributions of all measured rotations for all patients in study for each axis.

Figure 3a & 3b. Proportion of patients spending at least a given proportion of time within rotations resulting in acceptable PTV and CTV DVH results respectively for each axis of rotation.

Table 1. Mean, standard deviation and range of all KIM measured data for each rotation axis

Table 2: Mean and standard deviation of sphericity and conformity index across all patient for CTV and PTV along with number of patients spending at least 90% of their treatment within rotation angles resulting in acceptable DVH results.